

1. The first step is to identify the problem or question that needs to be answered. This involves understanding the context and the specific requirements of the task.

2. Next, gather relevant information and data. This may involve research, consultation with experts, or collecting data from various sources.

3. Once the information is gathered, analyze it to identify patterns, trends, and key factors that influence the outcome.

4. Based on the analysis, develop a plan or strategy to address the problem. This plan should outline the steps to be taken and the resources required.

5. Implement the plan and monitor the progress. It is important to stay flexible and adjust the plan as needed based on the results and feedback.

6. Finally, evaluate the outcome and draw conclusions. This involves comparing the results against the initial goals and objectives to determine the effectiveness of the solution.



# NASA CRUISE

# THERMAL CONDUCTIVITY OF COATED PARTICLE UO<sub>2</sub>-TUNGSTEN CERMETS

*Prepared by*

**Pleasanton, Calif.**

LOAN COPY: RETURN TO  
AFWL (WLIL-2)  
KIRTLAND AFB, N MEX

NATIONAL AERONAUTICS AND SPACE ADMINISTRATION • WASHINGTON, D. C. • AUGUST 1968



THERMAL CONDUCTIVITY OF COATED PARTICLE  
UO<sub>2</sub>-TUNGSTEN CERMETS

By L. N. Grossman

Distribution of this report is provided in the interest of information exchange. Responsibility for the contents resides in the author or organization that prepared it.

Prepared under Contract No. NAS 3-8511 by  
GENERAL ELECTRIC COMPANY  
Pleasanton, Calif.

for Lewis Research Center

NATIONAL AERONAUTICS AND SPACE ADMINISTRATION



## **FOREWORD**

The research described herein, which was conducted by the General Electric Company, was performed under NASA Contract NAS 3-8511 with Mr. Jack F. Mondt, Space Power Systems Division, NASA-Lewis Research Center, as Project Manager. The report was originally issued as General Electric Document GEST-2108.



## ABSTRACT

The thermal conductivity of cermets fabricated by hot-pressing of tungsten (W) coated uranium dioxide ( $\text{UO}_2$ ) was measured. Data obtained from specimens containing nominally 80 and 60 volume percent  $\text{UO}_2$  were compared with theoretical predictions based on Bruggman's model. Excellent agreement was found between theory and experiment in the 80 volume percent case in the temperature range of 900 to 1500°C. Less satisfactory agreement was obtained in the 60 volume percent case between 600 and 1700°C; the discrepancies could not be explained. The experimental technique, specimen preparation, experimental results and post-experiment metallography are presented.



## TABLE OF CONTENTS

	Page
ABSTRACT	v
SUMMARY	1
INTRODUCTION	2
EXPERIMENTAL TECHNIQUE	2
SPECIMEN PREPARATION AND CHARACTERIZATION	6
RESULTS AND DISCUSSION	11
CONCLUSIONS	21
References	22



## LIST OF FIGURES

Figure No.		Page
1	Radial Flow Thermal Conductivity Apparatus	3
2	Assembled Radial Flow Thermal Conductivity Apparatus	5
3	Neutron Radiographs of Platinum Sleeve and Cermet with Cadmium Wires in Thermocouple Holes	10
4	Experimental Thermal Conductivity	12
5	Experimental Thermal Conductivity	14
6	Comparison of Theory and Experiment for W-UO <sub>2</sub> Cermets	16
7	Photomicrographs of 80 Volume Percent Cermet	17
8	Uranium Metal in 80 Volume Percent Specimen	19
9	Photomicrographs of 60 Volume Percent Cermet	20

## LIST OF TABLES

Table No.		Page
I	Impurity Analyses of Coated and Uncoated Particles (ppm)	8
II	Characterization of Cermets	9

## SUMMARY

The thermal conductivities of nominally 80 and 60 volume percent  $\text{UO}_2$ -tungsten cermets have been measured for input into fuel element size and power density calculations. The cermets were fabricated by hot-pressing tungsten-coated  $\text{UO}_2$  spheres. The data obtained were compared with the theoretical predictions of Bruggeman's model for spheres dispersed in a continuous matrix.

The thermal conductivity of the 80 volume percent cermet was found to be 0.15 watt/cm- $^{\circ}\text{C}$  at 900 $^{\circ}\text{C}$  and 0.10 watt/cm- $^{\circ}\text{C}$  at 1500 $^{\circ}\text{C}$ ; a factor of five greater than bulk  $\text{UO}_2$ . Excellent agreement with theory was found for the 80 volume percent cermet. The experimental values of thermal conductivity for the 60 volume percent cermet did not agree well with predicted values. In that case, the experimental conductivity increased with temperature contrary to theory. The discrepancy could not be explained; however, thermocouple error could not be discounted.

Post-test examination of the cermet specimens revealed the initiation of  $\text{UO}_2$  penetration into tungsten grain boundaries. If this penetration continues in the cermet applications, the result could be a decrease in thermal conductivity to about 35% of the starting value.

## INTRODUCTION

Tungsten uranium dioxide (W-UO<sub>2</sub>) cermet s are being investigated for application as fuel for nuclear thermionic power sources. The choice of materials and fabrication procedures for the cermet fuel investigated in this program have been described in reference 1. Advantages of cermet fuel include lower thermal gradients, lower central temperatures in the UO<sub>2</sub> particles and the possibility of containing fission gas in the UO<sub>2</sub>. Accurate knowledge of the fuel thermal conductivity is prerequisite to nuclear reactor thermal design.

Predictions of thermal conductivity for composite materials based on existing theories have been recently reviewed in reference 2 by Miller. Bruggeman has derived a model in reference 3 for determining the conductivity of a discontinuous spherical phase surrounded by a continuous "matrix" phase which should be applicable to the cermets produced for this experiment. Part of this study was conducted to test the applicability of existing theories to the prediction of the high-temperature thermal conductivity of coated particle UO<sub>2</sub>-tungsten cermets.

## EXPERIMENTAL TECHNIQUE

A modification of the radial thermal conductivity flow technique (references 4 and 5) was used and Figure 1 is a schematic view of the apparatus employed. The specimen was a hollow cylinder 0.189-inch id, 0.510-inch od, and about one-inch long. The specimen was heated by a 0.090-inch tungsten central heater which was insulated from the cermet by a thoria tube. The tungsten heater was attached to water-cooled electrodes and heated by 400-cycle alternating current. Thermal expansion in the heater was compensated with a mercury-pool electrode at the lower end as shown in Figure 1. The container material for the mercury pool was made of molybdenum.

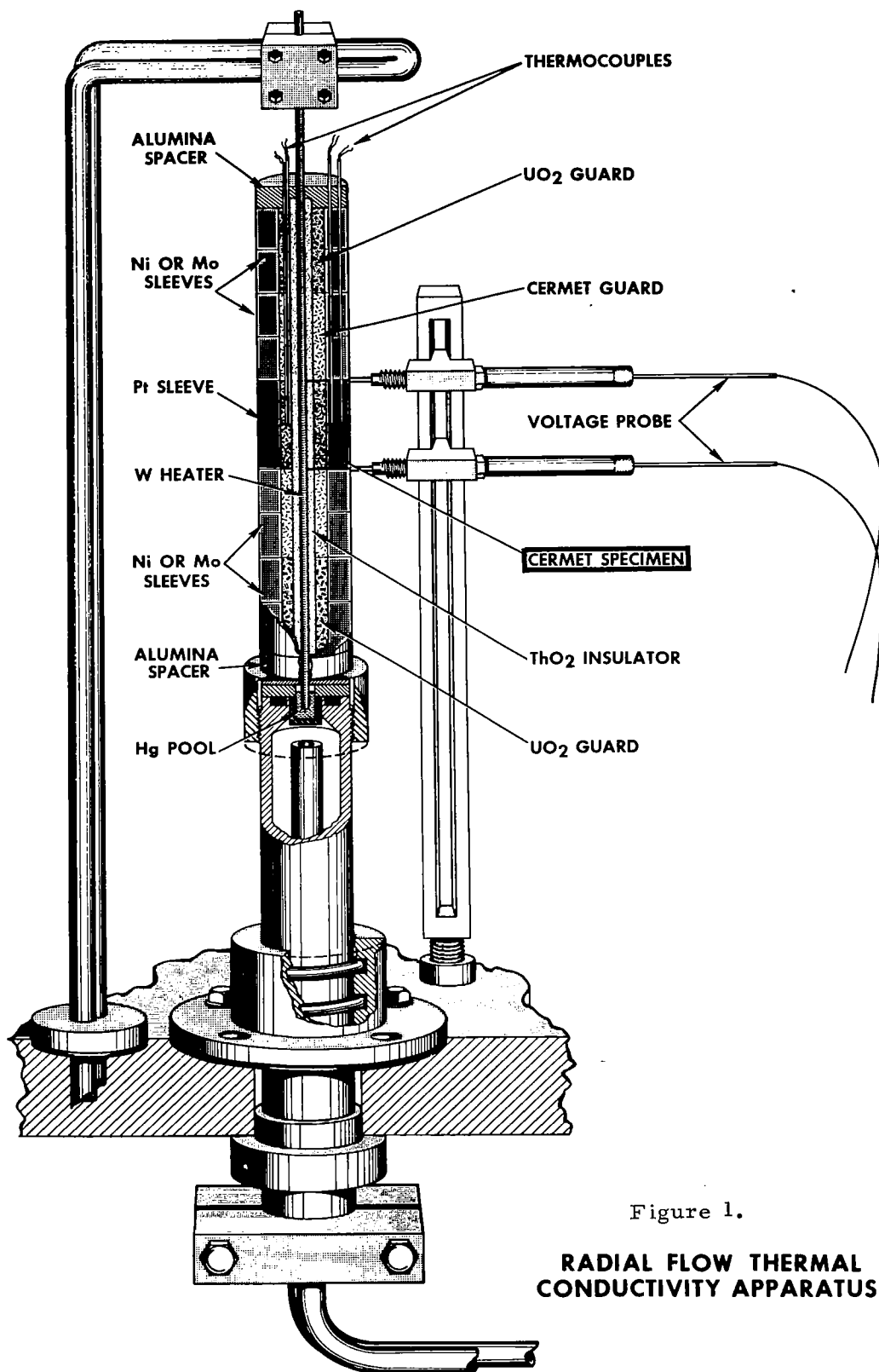


Figure 1.

**RADIAL FLOW THERMAL  
CONDUCTIVITY APPARATUS**

The tungsten rod was heated by a motor-generator (m-g) set whose output passed through a stepdown transformer. The m-g unit consisted of 10 HP, 3-phase, 3600 rpm, 440-volt induction motor driving a 400-cycle, single-phase, 120-volt generator. The transformer was a 5 KVA, 400-cycle, 120-volt input and 5-volt output. Heating current was measured by a Weston 327 current transformer coupled with a Weston 433 a-c Ammeter. The overall accuracy of current measurement was about one percent.

The specimen was thermally guarded longitudinally by two dummy cermets and by two  $\text{UO}_2$  insulators also shown in Figure 1. The guards were included to minimize longitudinal heat loss because the validity of the results depend directly on guarding efficiency. A length-to-diameter ratio of 4 has been shown in reference 6 to limit longitudinal losses to less than 5%. End losses are further reduced if narrow gaps exist between the specimen and guard interfaces as shown in reference 7.

Power into the cermet was measured by contacting the tungsten rod with two spring-loaded tungsten voltage probes. The probe leads were connected to a calibrated Tetronix 503 oscilloscope. Potential differences as low as 10 millivolts (R.M.S.) could be measured; the noise level was less than 0.1 millivolt; the waveform was perfectly sinusoidal.

An outer platinum sleeve was added to the usual radial flow device to provide a further measure of the heat flux. The known thermal conductivity (reference 8) and total hemispherical thermal emissivity (reference 9) of platinum provide two checks on longitudinal heat loss. A picture of the assembled apparatus is shown in Figure 2.

Measurements were carried out in vacuum. The pumping system consisted of a consolidated Electrodynamics Corp. Model PMC 721 oil diffusion pump, a W.M. Welsh Model 1397-B fore-pump, and a liquid nitrogen baffle-cryopump. Pressures were measured by a National Research Corp. Model 518 ionization guage. Typical pressure measured when the apparatus was in

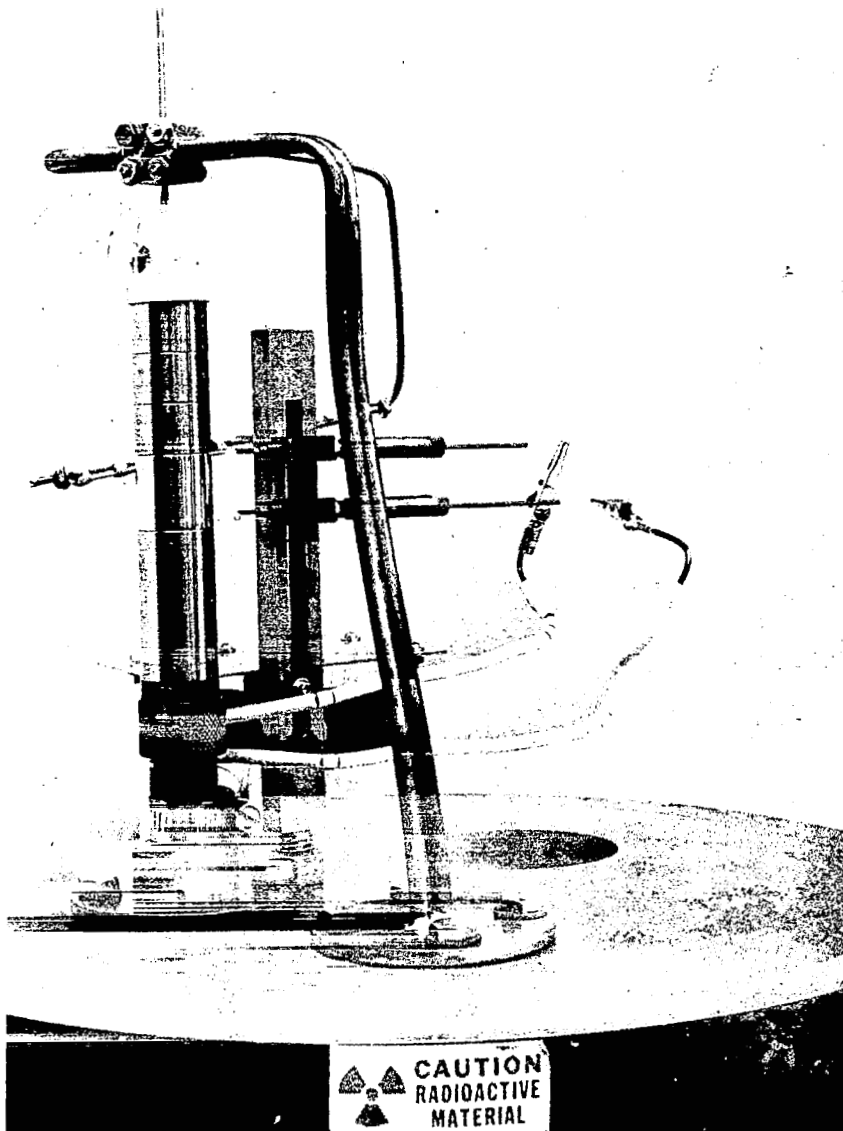


Figure 2. ASSEMBLED RADIAL FLOW THERMAL  
CONDUCTIVITY APPARATUS

operation was  $2 \times 10^{-6}$  torr. The high pumping speed of this vacuum system minimized specimen outgassing delays. The specimen stack could be observed through a four-inch diameter quartz window. The surface temperature profile of the platinum standard could be measured optically through the window.

Temperature measurements in the specimen and in the platinum sleeve was performed with W-5 Re vs W-26 Re and Pt vs Pt-10 Rh thermocouples, respectively. The W-5 Re vs W-26 Re couples were made from 0.005-inch Hoskins wire specially selected for homogeneity. The thermocouples were pretested in an isothermal furnace prior to experimentation. A maximum difference of  $7^{\circ}\text{C}$  was observed between selected W-Re couples at  $1900^{\circ}\text{C}$  and no drift was observed during four hours of comparison testing at  $1900^{\circ}\text{C}$ . Selected Pt-Rh couples were identical to within  $0.3^{\circ}\text{C}$  at  $1200^{\circ}\text{C}$  after four hours of comparison testing.

Thorium oxide was used to insulate the W-Re couples. The double-bore thoria tubing outside diameter varied between 0.036 and 0.040-inch. Aluminum oxide (Degussit A123) was used to insulate the Pt-Rh couples. Thermocouple beads were made by fusion in an argon-filled glove box for W-Re and in air for Pt-Rh. The beads were about 0.015-inch diameter in both cases. The thermocouples were insulated from the cermet and from the platinum sleeve by a small piece of thoria or alumina at the bottom of the thermocouple wells. The thermocouples were read independently on a Leeds and Northrup Model K-3 potentiometer; an ice-water bath served as the cold junction.

## SPECIMEN PREPARATION AND CHARACTERIZATION

Cermets were fabricated by vacuum hot-pressing W-coated  $\text{UO}_2$  spheres in graphite dies. The cermets were pressed at  $2050^{\circ}\text{C}$  and 11,000 psi for 10 minutes. The as-pressed cermets were 0.563 to 0.586-inch diameter and about one-inch long. They were centerless ground to 0.510-inch outside diameter to eliminate the carbon contamination which came from the graphite

dies, and then drilled with a high speed water-cooled diamond drill to 0.189-inch inside diameter. The specimen ends were ground flat by hand using a stainless steel holding jig and silicon carbide paper. Chemical analyses of the coated and uncoated  $\text{UO}_2$  particles are given in Table I. The coated cermet particles were  $100 \pm 10$  micron in diameter. Before coating, the  $\text{UO}_2$  spheres were of a density of  $10.5 \pm 0.2 \text{ gm-cm}^{-3}$ . Characterizations of the fabricated specimens are given in Table II. The specimen compositions given were determined by dissolution and total analysis for uranium and tungsten after testing. Two  $\text{UO}_2$  guards were fabricated in the same manner as the cermets except that they were pressed at  $1400^\circ\text{C}$  and 8000 psi for 15-minutes and slowly cooled to avoid cracking.

Holes to accommodate specimen thermocouples were drilled in the cermets with carbide drills. The thermocouple hole diameters were about 0.040-inch and penetrated about 1/2-inch into the specimens. Accurate thermocouple hole location was obtained by neutron radiography of the drilled cermets. Figure 3 is a neutron radiograph of an 80 volume percent  $\text{UO}_2$  cermet with cadmium wires inserted into the thermocouple holes. The platinum sleeve is also shown with cadmium wires in its thermocouple and voltage probe holes. Thermocouple position data in Table II were obtained from neutron radiographs. Thermocouples were assumed to be centered in their holes. This is believed accurate because of the care used in centering thermocouple beads in their wells with the aid of a hole in the small insulator just below the thermocouple.



TABLE I. Impurity Analyses of Coated and Uncoated Particles (ppm)

Element	"60 vol. %"		"80 vol. %"	
	Uncoated	Coated	Uncoated	Coated
	<u>UO<sub>2</sub></u>	<u>with W</u>	<u>UO<sub>2</sub></u>	<u>with W</u>
Ag	<0.1	<0.1	<0.1	<0.1
Al	24	12	54	<4
B	<0.2	<0.2	0.8	1.6
Bi	<1	<1	1	<1
Ca	5	20	<2	<2
Cd	<1	<1	< .5	< .5
Co	<2	<2	<2	<2
Cr	12	24	8	76
Cu	0.5	2	1.4	10
Fe	<14	14	8	16
Li	<0.5	<0.5	< .5	< .5
Mg	4	2	2	2
Mn	0.5	1	1	4
Mo	5	50	90	22
Na	<15	<15	2	8
Nb	0.02	<0.01	<1	<1
Ni	5	48	2	24
Pb	1	20	1	4
Si	<6	6	12	12
Sn	1	1	1	2
Ti	0.2	<0.01	10	10
Zn	<10	<10	<10	<10
Zr	0.2	<0.01	<1	<1
V	<11	<11	<11	50
Dy	<0.2	<0.2	<0.05	<0.05
Ea	<0.1	<0.1	<0.02	<0.02
Gd	<0.2	<0.2	<0.05	<0.05
Sm	<1	<1	<0.02	<0.02
C	16 $\pm$ 5	<5	19 $\pm$ 5	13 $\pm$ 5
Cl	3 $\pm$ 3	9 $\pm$ 3	3 $\pm$ 3	5 $\pm$ 3
F	5 $\pm$ 5	29 $\pm$ 5	5 $\pm$ 5	6 $\pm$ 5
N	<10	21 $\pm$ 10	5 $\pm$ 5	287 $\pm$ 25

Tolerances are +50%-25% unless otherwise stated.

TABLE II. Characterization of Cermets

	<u>"60 vol. %"</u>	<u>"80 vol. %"</u>
Density	13.92 gm/cm <sup>3</sup>	12.61 gm/cm <sup>3</sup>
Weight % W	55.17 wt %	34.05 wt %
Weight % UO <sub>2</sub>	44.83 wt %	65.95 wt %
Theoretical Density	14.39 gm/cm <sup>3</sup>	12.85 gm/cm <sup>3</sup>
% of Theoretical Density	96.7%	98.1%
Volume % W	39.8 vol. %	22.2 vol. %
Volume % UO <sub>2</sub>	56.9 vol. %	75.9 vol. %
Volume % Voids	3.3 vol. %	1.9 vol. %
O-to-U Ratio	2.00	2.00
Radial Position of Thermocouples (at Room Temperature)	r <sub>1</sub> = 0.318±.005 cm r <sub>2</sub> = 0.488±.005 cm	r <sub>1</sub> = 0.362±0.005 cm r <sub>2</sub> = 0.550±0.005 cm

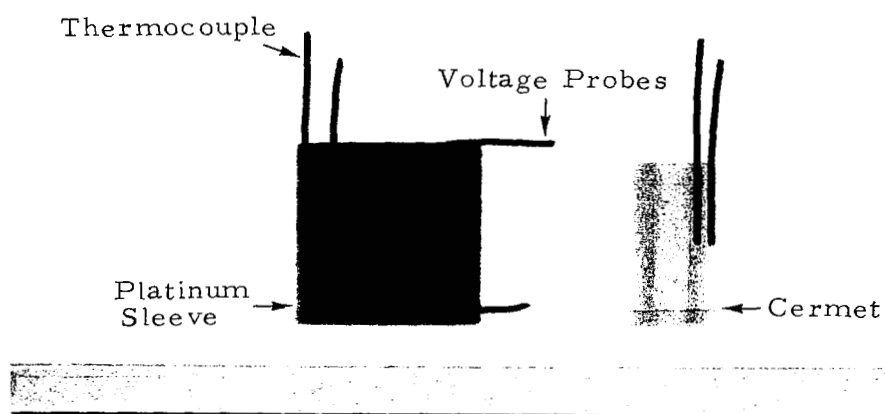


Figure 3. NEUTRON RADIOGRAPHS OF PLATINUM SLEEVE AND CERMET WITH CADMIUM WIRES IN THERMOCOUPLE HOLES

## RESULTS AND DISCUSSION

The thermal conductivity of the nominal 80 volume percent  $\text{UO}_2$ -tungsten specimen was determined first. The data were obtained over a period of about two days. The results are plotted in Figure 4 with thermal conductivity as a function of temperature. The measurements were reproducible and no changes in the measured data were observed over the two-day period. The thermal conductivity decreased with an increase in specimen temperature as expected. The temperature of the specimen was limited to  $1500^\circ\text{C}$  due to evaporation of the nickel sleeves located above and below the platinum sleeve. The evaporated nickel would condense on the thermocouple insulator surfaces and eventually cause the thermocouple to short. The 80 volume percent run was terminated when the highest temperature W-5 Re/W-26 Re thermocouple reading was  $30^\circ\text{C}$  lower in temperature than the predicted temperature from optical measurements. Cooling the specimen to below  $1200^\circ\text{C}$  would restore the thermocouple to its previous performance, but the apparent short would reoccur at about  $1600^\circ\text{C}$ . Disassembly of the apparatus revealed no structural nor chemical changes except evaporation of nickel (as previously described) and thoria from the top of the experimental stack.

The nickel sleeves were replaced with molybdenum sleeves before conducting the experiment containing the nominal 60 volume percent  $\text{UO}_2$ -tungsten specimen. This change allowed data to be taken up to a temperature of  $1650^\circ\text{C}$ . However, the tungsten voltage probes proved unreliable at specimen temperatures above  $1400^\circ\text{C}$  for both experimental runs. The failure mode was apparently loss of contact between one of the probes and the heater. The correlation between the heat input, as determined from current and probe voltage measurements, and the heat radiated, as determined from the platinum temperature and emissivity measurements was good. The calculated heat loss by radiation from the platinum was always within  $\pm 20\%$  of the heat input from the probe data and was randomly scattered. The heat input as determined from the temperature drop across the platinum was only accurate to about  $\pm 50\%$  because of the small temperature gradients. Therefore, the thermal

## EXPERIMENTAL THERMAL CONDUCTIVITY

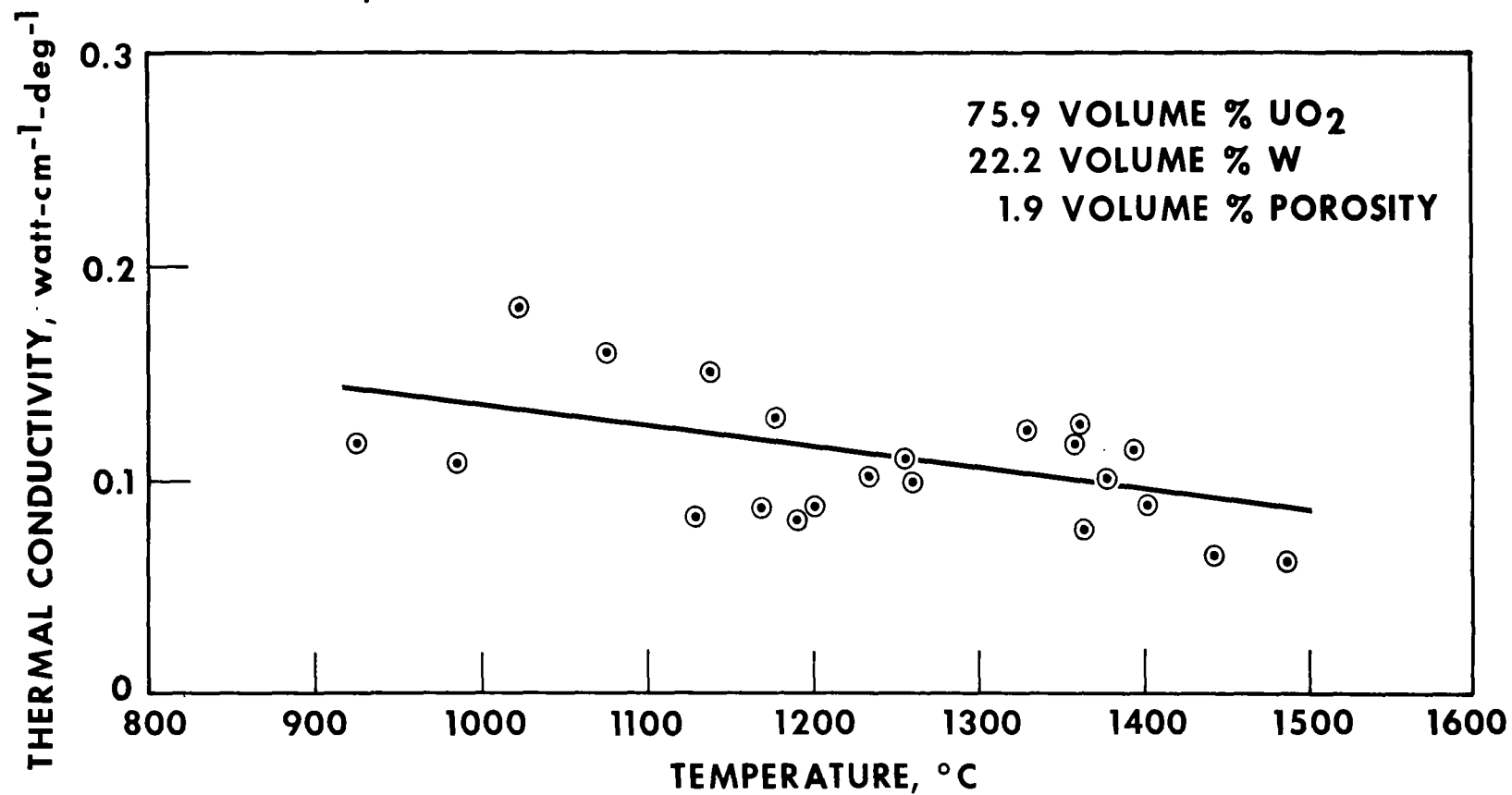


Figure 4.

conductivity for the high temperature region (above 1400°C) was determined from the calculated heat loss by radiation rather than the heat input values from the probe data.

The thermal conductivity of the 60 volume percent  $\text{UO}_2$ -tungsten cermet is shown on Figure 5 as a function of cermet temperature. The thermal conductivity increased with specimen temperature, which was not expected. Also, there was a noticeable change in the cermet thermal conductivity after the specimen had been at temperature for about 30 hours. The thermal conductivity data points at different temperatures before and after the 30 hours at temperature is also shown in Figure 5; however, the increase in conductivity with temperature was still apparent.

The experimentally determined conductivities were compared with those predicted by Bruggeman's theory. Bruggeman's theory should be valid in predicting conductivities of coated-sphere cermets, due to the continuity of the tungsten metal around the  $\text{UO}_2$  particles. The thermal conductivities of the 60 and 80 volume percent cermet specimens were calculated using the following equation from reference 4 for a dispersion of spheres.

$$f = \frac{K_D - K}{K_D - K_C} \sqrt[3]{\frac{K_C}{K}}$$

where

- K = Conductivity of the cermet
- $K_D$  = Conductivity of the  $\text{UO}_2$
- $K_C$  = Conductivity of the tungsten
- f = Volume fraction of the tungsten

The thermal conductivity used in the calculations is from reference 11 for  $\text{UO}_2$  and from reference 12 for tungsten. Since the porosity existed primarily in the  $\text{UO}_2$  material, it was accounted for in the  $\text{UO}_2$  conductivity.

## EXPERIMENTAL THERMAL CONDUCTIVITY

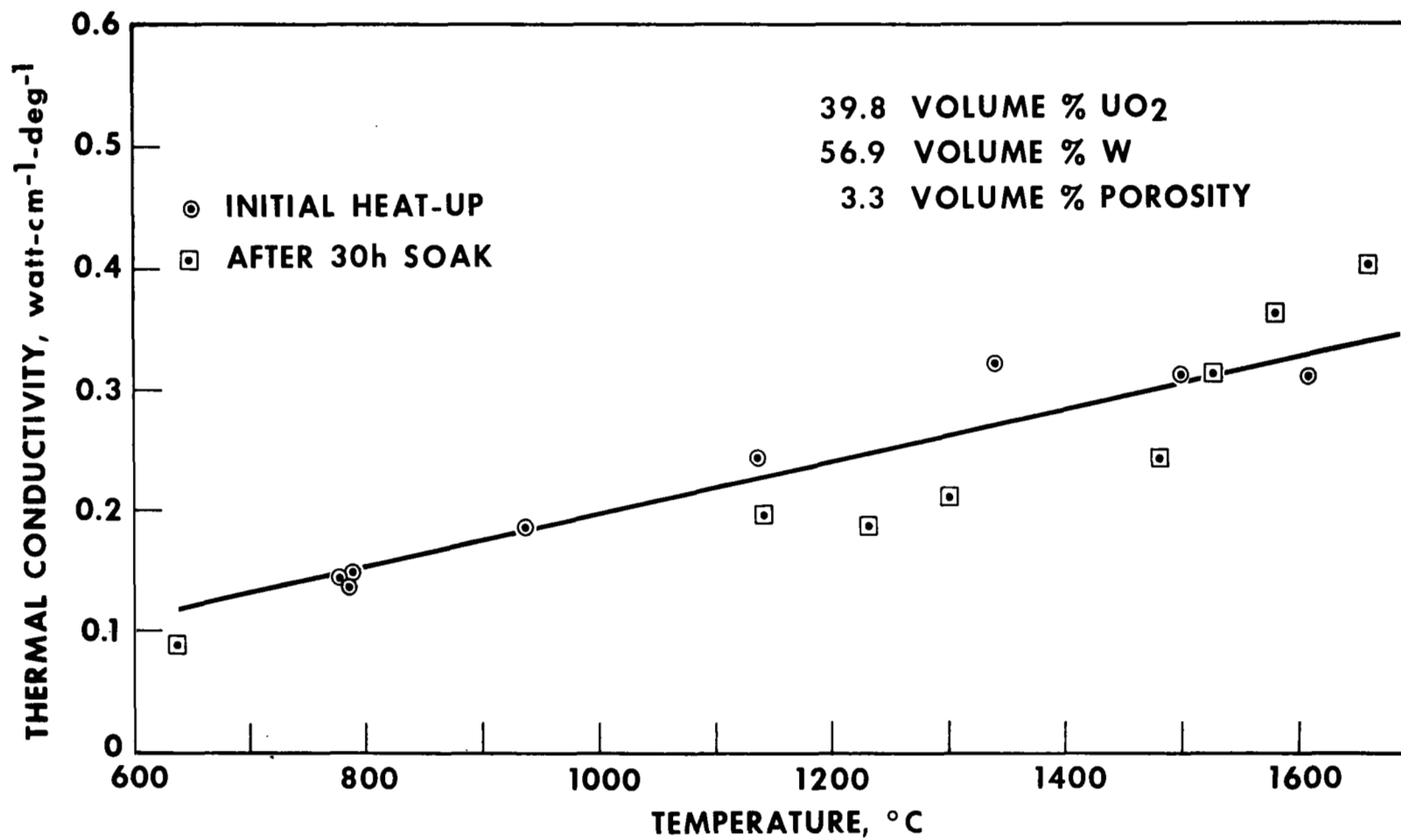


Figure 5.

The calculated and experimental conductivities are plotted as a function of temperatures in Figure 6. The curves are labeled E for experimental values and T for calculated values. The agreement is excellent for the 80 volume percent cermet. The experimental conductivity of the 60 volume percent has a positive temperature coefficient, while theory predicts a negative coefficient. The magnitude of the measured conductivity near the 1600°C temperature is higher than the theory allows. The discrepancy between theory and experiment is greater than the experimental error, assuming the thermocouples were within the original calibration error.

The possibility of thermocouple decalibration during the experimental testing of the 60 volume percent specimen cannot be discounted because the inner high temperature thermocouple failed during the final stages of testing and could not be post test calibrated. An inner thermocouple indicating a temperature lower than the actual temperature could cause the experimentally determined thermal conductivities to be higher than actual and could also cause an erroneous indication of a positive temperature coefficient.

An increase in thermal conductivity of a cermet with an increase in temperature was reported by Feith in reference 13 for a 60 volume percent  $\text{UO}_2$ , 40 volume percent molybdenum cermet fabricated from coated spheres. The theory predicts a decrease in conductivity with an increase in temperature for both the  $\text{UO}_2$ -molybdenum cermet and the  $\text{UO}_2$ -tungsten cermet. There was no published reason for the conductivity increase with temperature, although fabrication variables were identified as possible points of departure from the theory.

After obtaining the data and determining the thermal conductivity, the specimens were sectioned for metallographic analyses. Representative photomicrographs of the 80 volume percent  $\text{UO}_2$ -tungsten cermet are shown in Figure 7. It can be seen from the photomicrographs (Figure 7a) that the total cermet porosity of 1.9 volume percent is primarily in the  $\text{UO}_2$  region. The  $\text{UO}_2$  spheres have been slightly flattened in the longitudinal direction



## COMPARISON OF THEORY AND EXPERIMENT FOR W-UO<sub>2</sub> CERMETS

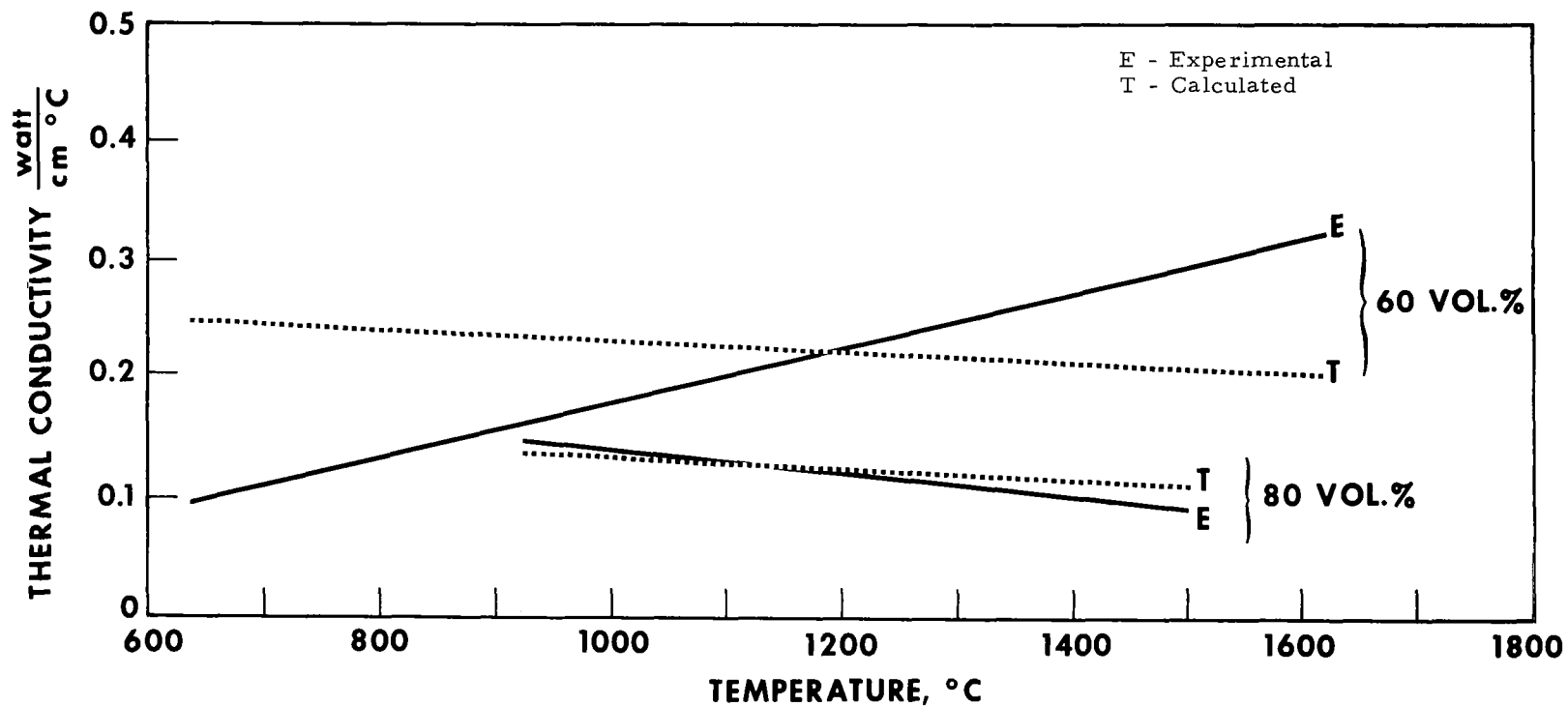
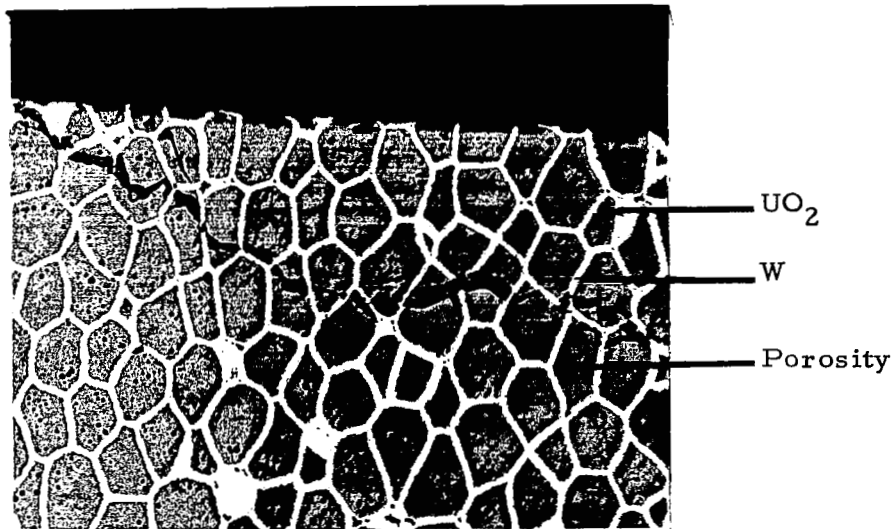


Figure 6.



- a. Longitudinal section, outside diameter (crack occurred during metallographic sectioning). Note porosity principally in  $\text{UO}_2$ ; also note slight flattening of fuel spheres. 100X



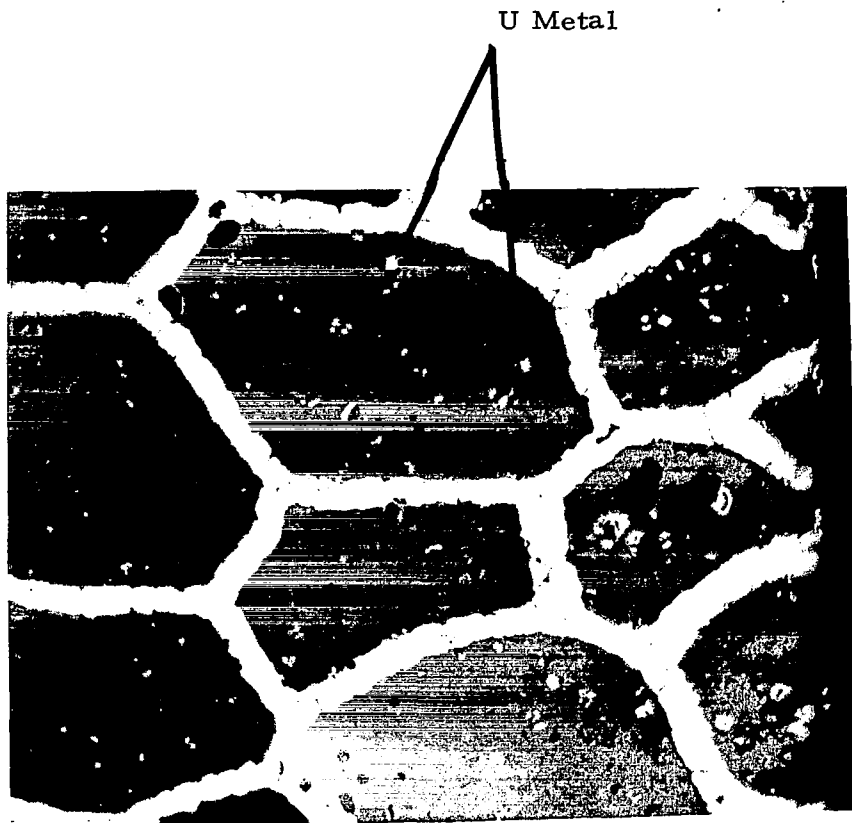
- b. Central area showing penetration of  $\text{UO}_2$  into W grain boundaries. 500X

Figure 7. PHOTOMICROGRAPHS OF 80 VOLUME PERCENT CERMET

because of hot pressing in that direction. Figure 7b illustrates the penetration of  $\text{UO}_2$  fuel into the tungsten grain boundaries after being held at high temperatures for about 50 hours. Some uranium metal was identified in isolated areas of the 80 volume percent cermet and a typical area is shown in Figure 8.

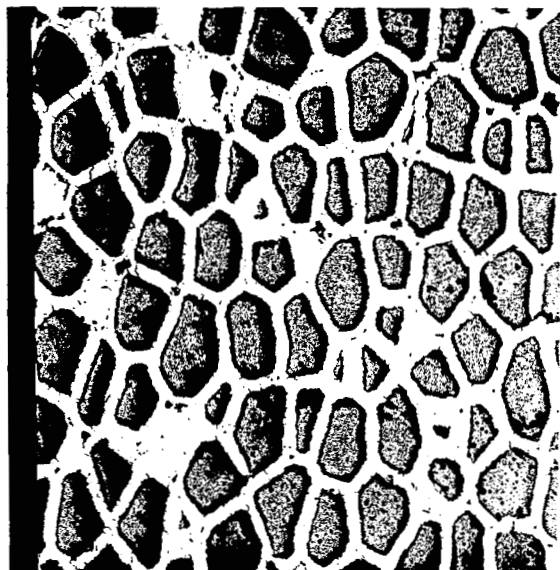
The 60 volume percent specimen was carefully examined for uranium metal and none was found. Photomicrographs of the 60 volume percent  $\text{UO}_2$ -tungsten cermet show that the same general characteristics are found in the 60 volume percent cermet as was found in the 80 volume percent cermet. These characteristics are: porosity principally in the  $\text{UO}_2$ , the  $\text{UO}_2$  spheres slightly flattened in the direction of hot pressing and penetration of  $\text{UO}_2$  into the tungsten grain boundaries after high temperature exposure. Those representative photomicrographs showing the above characteristics are included in Figure 9.

The  $\text{UO}_2$  penetration is accentuated by thermal cycling and could possibly result in complete isolation of the W grains after repeated severe cycling. Under those conditions where the W phase is no longer continuous, the Bruggeman equation for spheres dispersed in a continuous matrix would no longer be applicable. Under those conditions, the cermet conductivity would be lower and might better be represented by the Bruggeman Mixture Equation for Spheres. The result of a microstructural change from continuous to discontinuous tungsten in the 80 volume percent case is predicted to be a decrease in the cermet conductivity of about 35% of the starting value.

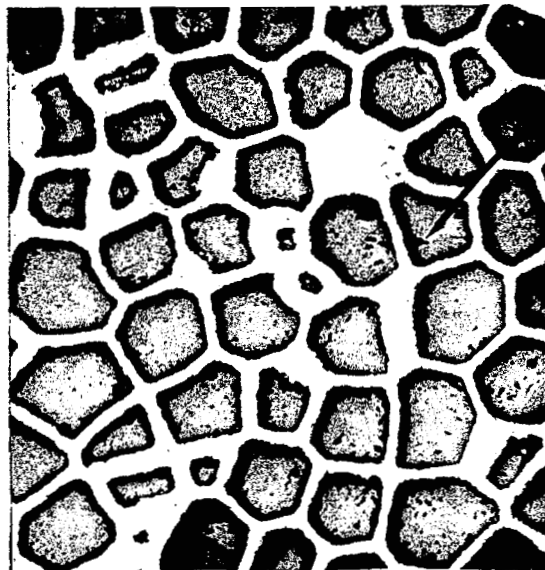


Outside Diameter; A typical area showing  
uranium metal. 500X

Figure 8. URANIUM METAL IN 80 VOLUME PERCENT  
SPECIMEN

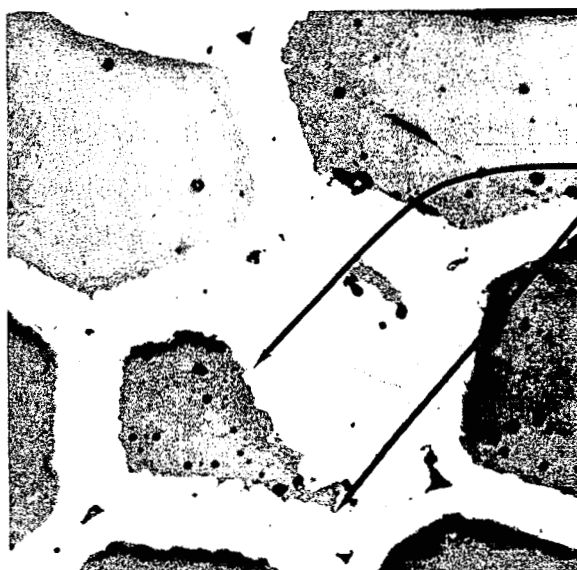


a. Longitudinal section. 100X  
Note slight flattening of spheres in pressing direction.



UO<sub>2</sub>  
Porosity

b. Transverse section. 100X  
Note location of porosity principally in UO<sub>2</sub>.



Penetration

c. Showing partial penetration of UO<sub>2</sub> into W grain boundaries. 500X

Figure 9. PHOTOMICROGRAPHS OF 60 VOLUME PERCENT CERMET

## CONCLUSIONS

The following conclusions were reached after conducting the experimental investigation of thermal conductivity of 80 and 60 volume percent  $\text{UO}_2$ -tungsten cermets.

1. The thermal conductivity of the 80 volume percent  $\text{UO}_2$ -tungsten cermet decreased linearly from 0.15 watt/cm- $^{\circ}\text{C}$  at 900 $^{\circ}\text{C}$  to 0.10 watt/cm- $^{\circ}\text{C}$  at 1500 $^{\circ}\text{C}$ .
2. The experimentally determined conductivities of the 80 volume percent cermet are in excellent agreement with those predicted by Bruggeman's theory for a dispersion of spheres in a continuous matrix.
3. The conductivity determined by experiment for the 60 volume percent cermet has a positive temperature coefficient, while theory predicts a negative coefficient based primarily on the negative coefficient observed for pure tungsten. The discrepancy between theory and experiment is greater than the experimental uncertainty, but the source of the discrepancy is unknown. Thermocouple decalibration is a possible source, because calibration was not possible after the experiment due to failure of the inner thermocouple during testing.
4. The initiation of uranium dioxide penetration into the tungsten grain boundaries was apparent in both cermet specimens after high temperature testing.
5. The cermet porosity was primarily in the  $\text{UO}_2$ .
6. The  $\text{UO}_2$  spherical particles were slightly flattened in the direction of hot pressing.

## REFERENCES

1. M.O. Marlowe, R.E. Ekvall, A.I. Kaznoff, "Development and Evaluation of  $\text{UO}_2$ -W Cermet Fuel for Nuclear Thermionic Emitters," NASA CR 72274, July, 1967, CRD.
2. J.V. Miller, "Estimating Thermal Conductivity of Cermet Fuel Materials for Nuclear Reactor Application," NASA TN D-3898, April, 1967, Unclassified.
3. D.A.G. Bruggeman, "Dielectric Constants and Conductivities of Aggregates of Isotropic Materials," *Ann. Physik*, 24, 636-679 (1935).
4. R.J. Runck, "Thermal Conductivity," in High Temperature Technology, I.E. Campbell, editor, J. Wiley and Sons, Inc., NY, 1956, 439-440.
5. T. Nishijima, T. Kawada, A. Ishihata, *J. Am. Cer. Soc.* 48, 31 (1965).
6. G.A. Slack, C.J. Glassbrenner, *Phys. Rev.* 120, 782 (1960).
7. A.D. Feith, "Measurements of the Thermal Conductivity and Electrical Resistivity of Molybdenum," in Fifth Conference on Thermal Conductivity, published by Denver Univ., Dept. of Metallurgy (1965).
8. M.J. Laubitz, M.P. vanderMeer, *Canadian J. Phys.* 44, 3173 (1966).
9. G.L. Abbott, N.J. Alveres, W.J. Parker, "Total Normal and Total Hemispherical Emittance of Polished Metals - Part II," WADD-TR-61-94, Part II; January, 1963.
10. U.E. Wolff, D.M. Rooney, "Metallic Inclusions in  $\text{UO}_2$ ," ORNL-TM-1161, p 249, February, 1966.
11. M.F. Lyons, G.E. Co. Report GEAP-4624, July, 1964.
12. V.S. Gumenyuk, V.V. Lebedev, "Investigation of the Thermal and Electrical Conductivities of Tungsten and Graphite," *Fiz. Metallov and Metallovedenige*, 2, 29, 1961 (Translated in USAEC-NP-TR-733).
13. J.F. Collins, P.N. Flagella, "Fabrication and Measurement of Properties of Mo- $\text{UO}_2$  Cermets," Figure 7, GEMP-545 (1967).